Chemosphere 352 (2024) 141410

Contents lists available at ScienceDirect

Chemosphere

journal homepage: www.elsevier.com/locate/chemosphere

Fine micro- and nanoplastics concentrations in particulate matter samples from the high alpine site Sonnblick, Austria

Daniela Kau [a,*], Dušan Materić [b,c,**], Rupert Holzinger [b], Kathrin Baumann-Stanzer [d], Gerhard Schauer [d], Anne Kasper-Giebl [a]

[a] Institute of Chemical Technologies and Analytics, TU Wien, Getreidemarkt 9, 1060, Vienna, Austria
[b] Institute of Marine and Atmospheric Research Utrecht, Utrecht University, Princetonplein 5, 3584CC, Utrecht, the Netherlands
[c] Department for Analytical Chemistry, Helmoltz Centre for Environmental Research – UFZ, Permoserstraße 15, 04318, Leipzig, Germany
[d] Geosphere Austria, Hohe Warte 38, 1190, Vienna, Austria

HIGHLIGHTS

- Fine micro- and nanoplastics were determined at a high alpine site in two seasons.
- Average plastics concentrations were 35 ng m^{-3} for PM_{10} and 21 ng m^{-3} for PM_1.
- Contribution of plastics to organic matter was comparable to an urban site.
- In winter/spring, plastics were mainly present as nanoplastics.

GRAPHICAL ABSTRACT

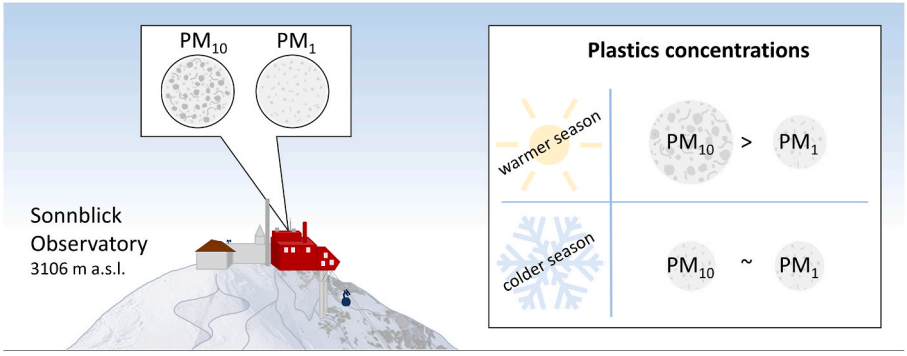

ARTICLE INFO

Handling Editor: Michael Bank

Keywords:
Particulate matter
Microplastics
Nanoplastics
High alpine environment
Mineral dust

ABSTRACT

We report atmospheric fine micro- and nanoplastics concentrations from particulate matter (PM) samples of two size fractions (PM_{10}, fine micro- and nanoplastics, and PM_1, nanoplastics), which were collected at the remote high alpine station Sonnblick Observatory, Austria. Active sampling was performed from June 2021 until April 2022. Analysis was done using TD-PTR-MS to detect 6 different plastic types. Polyethylene terephthalate (PET), polyethylene (PE) and polypropylene/polypropylene carbonate (PP/PPC) were found to be the dominating species. PET was detected in almost all samples, while the other plastic types occurred more episodically. Furthermore, polyvinyl chloride (PVC), polystyrene (PS) and tire wear particles were detected in single samples. Considering the three main plastic types, average plastics concentrations were 35 and 21 ng m^{-3} with maximum concentrations of 165 and 113 ng m^{-3} for PM_{10} and PM_1, respectively. Average polymer concentrations were higher in the summer/fall period than in winter/spring. In summer/fall, PM_{10} plastics concentrations were higher by a factor of 2 compared to PM_1, while concentrations of both size classes were comparable in the winter/spring period. This suggests that in the colder season plastic particles arriving at the Eastern Alpine crests are mainly present as nanoplastics. The contribution of micro- and nanoplastics to organic matter at the remote

* Corresponding author.
** Corresponding author. Department for Analytical Chemistry, Helmoltz Centre for Environmental Research – UFZ, Permoserstraße 15, 04318, Leipzig, Germany.
E-mail addresses: daniela.kau@tuwien.ac.at (D. Kau), dusan.materic@ufz.de (D. Materić).

https://doi.org/10.1016/j.chemosphere.2024.141410
Received 16 November 2023; Received in revised form 22 January 2024; Accepted 6 February 2024
Available online 10 February 2024

site was found to be comparable to data determined at an urban site. We found significant correlations between the PET concentration and tracers originating from anthropogenic activities such as elemental carbon, nitrate, ammonium, and sulphate as well as organic carbon and arabitol.

1. Introduction

Global plastics production exceeded 390 million tonnes in 2021, polyethylene being the most abundantly produced (PE, 26.9%), followed by polypropylene (PP, 19.3%) and polyvinyl chloride (PVC, 12.9%). Plastic types with lower abundances include polyethylene terephthalate (PET, 6.2%) and (expandable) polystyrene (PS/PS-E, 5.3%) among others (PlasticsEurope, 2022). Compared to 235 million tonnes produced globally in 2011 (PlasticsEurope, 2012), this represents an increase of 66% within one decade. After their use, plastic products turn to waste and recycling rates are still low. In 2019, only 9% of global plastic waste was recycled, 19% was incinerated and almost 50% deposited in sanitary landfills, while the residual 22% was mismanaged plastic waste, which was disposed of in uncontrolled dumpsites, burnt in open pits or leaked into the environment (OECD, 2022). Annual global mismanaged plastic waste was estimated between 60 and 99 million tonnes in 2015 and projected to triple to 155 to 265 million tonnes per year by 2060 in a business-*as*-usual scenario (Lebreton and Andrady, 2019).

Plastic products are produced in different sizes and shapes and degrade over time. Andrady (2015) lists solar UV-induced photodegradation reactions, thermal reactions, hydrolysis, and microbial biodegradation as main processes for plastics degradation in the ocean, exposure to UV light being the most powerful. Faster deterioration and fragmentation of plastics was reported in air compared to soil, ultrapure water, or the marine environment (Cai et al., 2018; Napper and Thompson, 2019). Deterioration is not only conditional on the environment (air, seawater), but also on the plastic type and the amount of light (Biber et al., 2019). Biodegradation rates increase with decreasing size and increasing surface area of plastic particles (Chinaglia et al., 2018). A decrease in microplastics size accompanies an increase in particle number (Hale et al., 2020). According to DIN CEN ISO/TR 21960, large microplastics comprise any solid, water insoluble plastic particles with dimensions between 1 and 5 mm, while dimensions of microplastics range between 1 μm and 1 mm and nanoplastic particles are smaller than 1 μm (DIN e.V, 2021). Based on this definition, samples evaluated within this study comprise fine microplastics and nanoplastics.

To date, there is no reference method for the analysis of micro- and nanoplastics. Hence, a wide variety of analytical methods is currently employed and both particle-based (e.g., μ-FTIR and μ-Raman) and mass-based (e.g., Py-GC-MS and TD-PTR-MS) methods are regularly used (Ivleva, 2021). Limitations of different analytical methods comprise problems regarding smallest determinable particle size (Chen et al., 2020), sampling substrate (Wright et al., 2019), low or unknown recoveries (Materić et al., 2020) and inadequate libraries for identification (Araujo et al., 2018).

Literature on environmental micro- and nanoplastics mainly refers to the aquatic and terrestrial compartments (e.g., Kumar et al., 2020; Rodrigues et al., 2018). The relevance of understanding airborne microplastics is pointed out by the increase in studies on the topic and is mentioned explicitly in reviews (e.g., Chen, G. et al., 2020; Kacprzak and Tijing, 2022) and in the context of recognizing inhalation as an important pathway for human uptake, that may lead to adversary health effects (Cox et al., 2019; Prata, 2018). Studies report airborne plastics in both urban (e.g., Akhbarizadeh et al., 2021; Jiang et al., 2024; Kirchsteiger et al., 2023) and remote sites (e.g., Abbasi and Turner, 2021; Allen et al., 2022; Brahney et al., 2020), most of them analysing concentrations after deposition rather than actual ambient concentrations. Especially data on airborne nanoplastics is still hardly available due to analytical limitations as mentioned above.

Since micro- and nanoplastics were detected not only in densely populated areas but also in remote regions including the polar regions (e.g., in snow, Bergmann et al., 2019, or sea ice and seawater, Kanhai et al., 2020) and various high-altitude mountains in different environmental matrices including sediments, snow, ice cores as well as biological samples (e.g., Cabrera et al., 2020; Materić et al., 2021; Pastorino et al., 2021), long-range atmospheric transport of those particles is discussed. Studies reporting aerosol concentrations indicate that they can be transported over distances above 1000 km (González-Pleiter et al., 2021; Wang et al., 2020). The special need for data of microplastics in the sensitive high-altitude environments is discussed in detail in the review by Padha et al. (2022).

Here, we (1) provide a first set of atmospheric fine micro- and nanoplastics data for the remote high alpine site Sonnblick in central Europe in two seasons (summer/fall and winter/spring), (2) compare micro- and nanoplastics concentrations in two size fractions (fine microplastics and nanoplastics) and (3) assess correlations between plastics concentrations and the occurrence of other constituents of particulate matter.

2. Materials and methods

2.1. Sampling, transport, and storage

Particulate matter of two size fractions (aerodynamic diameter $\leq$10 μm, PM_{10}, and $\leq$1 μm, PM_1) was sampled parallel onto quartz fibre filters (Pallflex® Tissuquartz™) at the remote high alpine GAW (Global Atmosphere Watch) station Sonnblick Observatory (3106 m a.s.l.), Austria. Sample change was performed weekly. Active sampling of PM_{10} was performed with a high-volume sampler (DIGITEL DH-77), while PM_1 was collected via low-volume sampling. Thus, actual mass concentrations in ambient air could be calculated, representing concentrations inhaled when staying at the site. Field blanks were available for both size fractions and were treated in the same way as the sample filters.

23 weekly filters and 5 field blanks of each size fraction were selected for analysis, leading to an overall number of 56 samples. The weekly filters covered two periods, summer/fall (17.06.2021 to 15.09.2021, no data available for 19.08.2021 to 02.09.2021) and winter/spring (23.12.2021 to 07.04.2022, no data available for 30.12.2021 to 06.01.2022 and 27.01.2022 to 07.02.2022). The number of samples for both periods is similar (summer/fall: n = 11; winter/spring: n = 12). During these seasons several mineral dust events occurred, where dust mainly from the Saharan desert reached Sonnblick Observatory after long-range transport.

As sampling was part of a long-term monitoring project, transport and storage of PM_1 filters was done in sealed polystyrene petri dishes. Transport of PM_{10} filters was performed in air-tight metal containers. In the laboratory, aliquots for the analysis of plastics were taken using a metal punch and stored in prebaked aluminium foil. The residual filter was stored in polyethylene (PE) bags for further analyses (inorganic ions, carbonaceous compounds, metals). All samples were stored frozen until analysis. To assess the influence of the different storage methods on the microplastics concentration (contamination, loss of particles), aliquots of four randomly chosen samples and one field blank were stored for up to 8 months in aluminium foil and PE bags in parallel.

Total suspended particle mass (TSP) was determined using a β-attenuation monitor (SHARP-Monitor Model 5030, Thermo Scientific) installed subsequent to a whole air inlet. While the inlet is designed to

have an upper cut-off size of 20 μm aerodynamic diameter at a wind speed of 20 m/s, losses of particles >1 μm will occur (Schauer et al., 2016). Hence the classification of aerosol mass concentrations as TSP (total suspended particles) is a simplification and actual TSP concentrations will be underestimated.

2.2. Plastics analysis

2.2.1. Method description

For analysis via thermal desorption-proton transfer reaction-mass spectrometry (TD-PTR-MS), aliquots of PM_{10} and PM_1 filters with a diameter of 3 mm were put in prebaked 10 mL glass vials (250 °C over night; VWR screw neck vials) and dried at 50 °C for 4 h. Triplicate analyses of each sample filter and at least duplicate analyses of blanks (field blanks, material blanks and system blanks; for more details see section 2.2.2.) were performed.

Analysis of six plastic types (polyethylene, PE; polyethylene terephthalate, PET; polypropylene/polypropylene carbonate, PP/PPC; polystyrene, PS; polyvinyl chloride, PVC; tire wear, Tire) was performed via TD-PTR-MS (PTR-TOF 1000, IONICON Analytik). Vials (filled with sample filters) were placed in the thermal desorption unit (1.5 min at 35 °C, ramp with 40 °C min^{-1} to 360 °C, plateau at 360 °C for 3 min). The vial was flushed with purified air at a flow of 100 mL min^{-1}. A subflow of approximately 40 mL min^{-1} was led to the PTR-MS through a heated line (Restek sulfinert coated stainless steel, 1 mm inner diameter, 180 °C). The PTR-MS was operated at a pressure of 2.8 hPa, 120 °C, and an E/N of 105 Td. The acquisition rate for mass spectra was 1 s.

Raw data was processed with PTRwid (Holzinger, 2015; version PTRwid_v003_may_18_2022). Integration started at 200 °C, leading to an average mass spectrum for each measurement. Samples and field blanks were corrected using the average signals from the material blank measurements (n = 37) for each ion. The resulting data was compared to the limit of detection (LOD = threefold standard deviation) of material blank measurements, all signals from ions below the LOD were set to zero. The obtained mass spectrometry data was put in a previously described fingerprinting algorithm (Materić et al., 2020).

2.2.2. Quality assurance

The ubiquity of plastics and the extensive use of plastic products as sampling and laboratory equipment necessitates extensive quality assurance measures to avoid contamination. The filter material for PM_{10} collection was directly used, however, the outermost filters of the stack which are in contact with packaging material, were not employed to reduce risk of contamination. For PM_1 collection, the filter material was prebaked at 450 °C for 24 h in a muffle furnace and cooled in a desiccator above distilled water. All equipment and the laminar flow bench, in which sample preparation was conducted, were accurately cleaned with HPLC grade water. We analysed field blanks, material blanks and system blanks on each measurement day. Material blanks (Pallflex® Tissuquartz™, baked at 450 °C for 3 days) were prepared to account for the quartz fibre material, while system blanks (prebaked empty glass vials) were run to evaluate the instrument's overall performance. Field blanks, which were prepared, transported, and stored as the filter samples, were analysed to indicate possible contamination in the overall process.

PM_{10} and PM_1 field blanks were evaluated separately due to the difference in sample preparation and storage. Only PET was detected in field blanks in 1 of 16 analyses for PM_1 and in 2 of 15 analyses for PM_{10}, leading to low average concentrations of 0.17 ng and 0.27 ng and LODs of 2.1 ng and 2.6 ng for PM_1 and PM_{10}, respectively. These average PET masses of blanks were subtracted from sample results. All samples that showed a significant match score during fingerprinting were above the LOD. No significant match score was obtained during the fingerprinting for 1 and 4 samples for PM_{10} and PM_1, respectively. Using the average air volume and loaded areas of filters, the average PET masses on field blanks correspond to 0.07 ng m^{-3} and 0.17 ng m^{-3} for PM_1 and PM_{10}, respectively. For comparison, if PET was detected on filters, ambient concentrations after blank correction ranged from 4.10 to 29.5 ng m^{-3} for PM_1 and 0.53–35.6 ng m^{-3} for PM_{10}.

Filter aliquots stored in prebaked aluminium foil and PE bags were analysed and compared. The field blank did not show signals for any of the analysed plastics, independent of the storage method. The loaded samples showed signals only for PET, with no statistically significant differences between PET loadings of samples stored in aluminium foil or PE bags. Therefore, we conclude that no contamination with plastics and no detectable loss of PET particles occurred when storing the filters in PE bags compared to aluminium foil. While this comparison could only be done for PET, as no other plastic types were present on the randomly chosen filters, we still do not expect loss of particles for any of the other plastic types. This allows to analyse also archived samples of the time series, which were stored frozen in PE bags, in the future. Further information can be found in the Supplement.

To assess influences of the sample matrix on the detection of plastics via TD-PTR-MS, a diluted PS standard (Particle Size Standard 1.046 μm, 2% w/v aqueous suspension, micro particles GmbH, Germany) was added to three aliquots of a filter with high particle loading and a filter with low particle loading as well as a field blank. Due to the higher availability (bigger loaded area and hence possibility to obtain several samples), these tests were conducted with aliquots of PM_{10} filters. Still, we assume that the results are representative for both fractions. For all analyses (n = 9), a distinct fingerprint match for PS was obtained. The recovery of PS was between 21 and 42% (averages: between 25 and 34%) and 31% on average, see Fig. S2 in the Supplement. This recovery is higher than previously reported for other sample types analysed with this method (see Supplement for more information). Limited ionisation efficiency and an uncertainty of ±60% was previously discussed for TD-PTR-MS (Materić et al., 2022). Due to the limited ionisation efficiency and the high uncertainty, the concentrations reported here for plastics are considered semi-quantitative and represent lower estimations of micro- and nanoplastics (Materić et al., 2020, 2021). No correction factor was applied to our results, as the recoveries for different plastic types are still unknown due to a lack of suitable standards (Holzinger et al., 2019; Materić et al., 2020).

Despite not being fully quantitative, TD-PTR-MS offers many advantages including high sensitivity and high mass resolution (Materić et al., 2017, 2019). For our samples, the quartz fibre filter substrate poses a limitation for optical methods, which are often applied for microplastics analysis. Wright et al. (2019) describe that they could not visualize microplastics on quartz fibre filters under a normal light microscope and as microplastics can be embedded in the quartz fibre matrix it is likely to be missed by Raman Spectral Imaging. The high temperature stability of the quartz fibre filter material allows to subject the samples to thermal desorption, which will also affect embedded particles. Apart from taking aliquots for analyses, no sample preparation was necessary. Hence, loss of particles is expected to be low (compared to washing out particles from substrates as required for other methods) and for our type of samples TD-PTR-MS is a suitable method for plastics analysis.

2.3. Other constituents of PM

Ion chromatography was used to quantify inorganic anions (NO_3^-, SO_4^{2-}), carbohydrates (levoglucosan, arabitol) and inorganic cations (NH_4^+, Ca^{2+}). For the quantification of inorganic anions and carbohydrates, filter aliquots were eluted in ultrapure water and analysed using a Dionex ICS 1100 and a Dionex ICS 3000 system (Thermo Scientific), respectively. To quantify inorganic cations, aliquots were eluted in 30 mM methanesulfonic acid and analysed using a Dionex Aquion system (Thermo Scientific).

Thermal-optical analysis was utilized to quantify organic carbon, OC, elemental carbon, EC, and total carbon, TC (TC = OC + EC), using a Lab OC/EC Aerosol Analyzer (Sunset Laboratory Inc.) and the EUSAAR2

protocol (Cavalli et al., 2010). OC was used to estimate organic matter, OM, on the sample filters using a conversion factor of 1.7 taken from Puxbaum et al. (2007). This conversion factor represents the overall PM composition and agrees well with the theoretical factor for pristine PET (1.6). Thermal-optical analyses of PET confirmed that it decomposes and desorbs in the inert atmosphere and hence is quantified as OC.

Inductively coupled plasma-optical emission spectroscopy was employed to quantify Fe after microwave-assisted digestion (Multiwave 5000, Anton Paar) of aliquots in Milli-Q water, HNO_3 and HBF_4 with the preinstalled method EN 13657. Further details regarding analytical methods are given in the Supplement.

2.4. Data evaluation

2.4.1. Source region analysis

The source region of particles was determined using the Lagrangian transport and dispersion model FLEXPART (Stohl et al., 2002) in backward mode on model-level analyses from the European Centre for Medium Range Weather Forecast with 1° × 1° resolution and 60 vertical layers, for the lowest 2000 m above ground level. More details are given in Baumann-Stanzer et al. (2019). The model results are given as source-receptor sensitivities (SRS), which reflect the source regions of air, sampled at the site during a defined time interval. Here this time interval was set to 3 h (9–12 a.m.), every day of filter sampling and the source regions of the previous 6 days, in respect to the arrival at Sonnblick, are considered.

Depending on the time of sample change, up to 8 SRS maps were assigned to every weekly sample. Generally, the rather long sampling intervals of one week are unfavourable for such evaluations, because they may cover rather different source areas due to changing weather patterns during the respective sampling period. To get more representative results, the individual SRS maps were weighted according to the TSP concentration prevailing at the site during the arrival of air masses and SRS maps with a contribution of less than 10% to the final aerosol loading were disregarded to further evaluation. This puts the focus on time periods which contribute most to average mass.

2.4.2. Statistical evaluation

Statistical data evaluation was conducted using DataLab (Epina GmbH, Austria; version 3.961; http://datalab.epina.at/). Spearman rank correlations of analysed parameters were examined for both the original and a standardized data set. For standardization, all ambient concentrations were divided by the respective TSP mass concentrations, as all parameters except levoglucosan showed a significant correlation with TSP mass. Correlation analysis of the standardized data set was limited to PM_{10} filters.

3. Results

3.1. Atmospheric micro- and nanoplastics concentrations

PET was identified as the most abundant type of plastics in the samples, followed by PE and PP/PPC. Tire wear particles, PS and PVC were rarely determined, and if this was the case with quite low concentrations. Interestingly, these plastics were identified only during winter/spring, making the overall plastics distribution more diverse during this period. Just one sample, collected between 24.03.22 und 31.03.22, showed marked concentrations of PVC in the PM_1 fraction. As noted in section 3.2., this sample was most likely influenced by fires occurring across several regions of Europe. No clear explanation can be given why the PM_{10} fraction collected simultaneously is not affected, leaving contamination as well as matrix effects as possible causes for this inconsistency.

An overview of ambient plastics concentrations determined for the time periods June to September 2021 and December 2021 to April 2022 is given in Fig. 1, with three gaps of one to two weeks marked with vertical dotted lines. Adjacent bars represent concentrations determined within the PM_{10} and PM_1 fraction, respectively. The error bars given in Fig. 1 represent the standard deviation of the triplicate analysis of filter aliquots. If more than one type of plastic was present, the combined standard deviation is shown. The data of ambient plastics concentrations (average and standard deviation of triplicate analysis) for each weekly sample are given in Table S1 in the Supplement, while the results of single measurements of all polymers can be found in the Supplementary Material (https://doi.org/10.48436/qfpa8-ga860).

As PET, PE and PP/PPC dominate the plastics concentrations, we focus further evaluations on these plastic types only. The average plastics concentrations were 35 and 21 ng m^{-3}, for the PM_{10} and PM_1 fractions. Maximum concentrations of 165 and 113 ng m^{-3} were reached for PM_{10} and PM_1, respectively. Generally, the agreement of the triplicate analysis, expressed as the relative standard deviation, was best for PET (PM_1: 8.8%; PM_{10}: 11%), while larger variation was found for PE (PM_1: 87%; PM_{10}: 90%) and PP/PPC (PM_1: 58%; PM_{10}: 91%), mostly due to the false-negative fingerprint of those plastics for some replicates.

Compared to $PM_{2.5}$ data of plastics from the city of Graz, Austria, obtained with the same analytical method, the average and maximum concentrations at Sonnblick are much lower (Graz: average 238 ng m^{-3}, maximum: 557 ng m^{-3} Kirchsteiger et al., 2023). This was expected as a

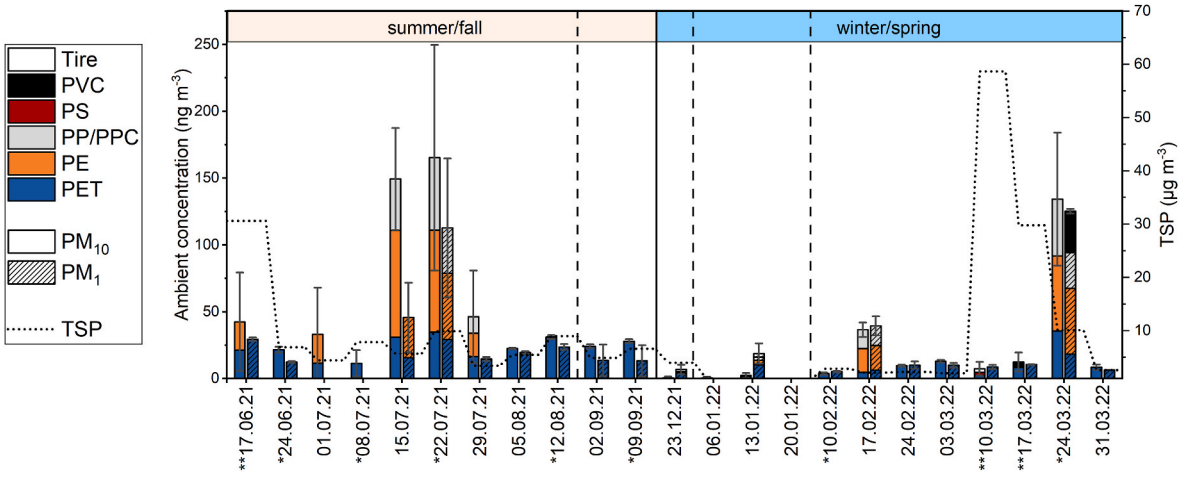

Fig. 1. Ambient fine micro- and nanoplastics concentrations (PM_{10} and PM_1) in chronological order, the given date is the start of sample collection. Discontinuities in the timeline are marked with a dotted line. Average values are shown, the error bars represent the standard deviation of triplicate analysis. Samples that were classified as influenced by mineral dust are labelled with *, strongest dust events are marked with **.

decrease of atmospheric microplastics from densely populated urban areas to rural areas was found over land and to the open ocean, and a vertical pollution concentration gradient with higher concentrations near the ground was suspected for microplastics along the lines of particulate matter (González-Pleiter et al., 2021; Prata, 2018; Wang et al., 2022). Time periods with maximum plastic concentrations do not follow maxima in concentrations of overall particulate matter mass (TSP), which are, as explained in more detail later (section 3.2.), mainly driven by transport of mineral dust. The contribution of plastics to overall aerosol mass could only be approximated, as mass concentrations of the PM_{10} and PM_1 fraction are not available. Still, plastics concentrations in the PM_{10} fraction could be related to TSP mass. Expressing these contributions on a percentage scale, this approximation gives values up to 2.5%, with an average of 0.59%. This is in quite good agreement with the average plastics contribution of 0.67% reported previously for the $PM_{2.5}$ fraction at an urban site in Austria (Kirchsteiger et al., 2023). As plastics comprise part of organic matter (OM), their contribution to OM is evaluated as well. Average OM concentrations in PM_{10} are 1.8 μg m^{-3} (maximum of 5.2 μg m^{-3}) and 1.5 μg m^{-3} (maximum of 3.4 μg m^{-3}) in PM_1. The share of plastics in OM was quite similar for both size fractions, with average values of 2.0% (PM_{10}) and 1.6% (PM_1). Again, these numbers are in quite good agreement with data from the city of Graz, Austria, with average plastics contributions to OM of 1.7% (Kirchsteiger et al., 2023). This suggests that micro- and nanoplastics are an equally important component in particulate matter in background regions compared to urban areas regarding mass contributions. Note that the samples were not collected at the same period, which may influence maximum contributions.

While PET was determined in all PM_{10} samples containing plastics (22 out of 23 samples), PE and PP/PPC occur more episodically and in 5 of 7 cases together. This is observable also in the PM_1 fraction, where PET was found in 19 of 23 PM_1 samples, again all samples containing any kind of plastics, while PE and PP/PPC are found more episodically (in 6 samples). PET concentrations show rather small variation across the entire sampling periods (summer/fall or winter/spring). Still, as PE and PP/PPC concentrations can be quite high, a marked increase in overall plastics concentrations is obtained for single weeks. This increase strongly affects the averages across the entire sampling periods.

The average fraction of each type of plastic to overall plastics mass is shown in Fig. 2. PET, the most abundant type of plastics, contributes 43 and 53% to plastics mass on PM_{10} and PM_1 filters, respectively. PE was the second most abundant type of plastics by mass, contributing 37 and 31% to plastics mass on PM_{10} and PM_1 filters, respectively. PP/PPC, the third most abundant type of plastics, contributes 20 and 16% to plastics mass on PM_{10} and PM_1 filters, respectively.

Average concentrations and relative contributions of different plastic types to overall plastics concentrations change when the different seasons are considered (Fig. 2). For the winter/spring period, the average plastics concentrations of both fractions (18 ng m^{-3} for PM_{10} and 17 ng m^{-3} for PM_1) and the contribution of the different plastics in both size fractions are well comparable. This shows that nanoplastics contribute substantially to plastics concentrations in the PM_{10} fraction during this period. In summer/fall, the average plastics concentrations reach higher up, with PM_{10} (52 ng m^{-3}) being a factor of 2 higher than PM_1 (26 ng m^{-3}). Furthermore, the relative contributions of plastics vary, when the two size fractions are considered. PE and PP/PPC are less abundant in the smaller fraction, leading to a higher relative contribution of PET.

The ratios of atmospheric plastics concentrations in summer/fall to winter/spring are 3 and 2 for PM_{10} and PM_1, respectively. This is in reasonable agreement with the ratios calculated for particulate sulphate and OM concentrations (PM_{10}: 2 and PM_1: 3 for both constituents). Such seasonal cycles for particulate matter have been determined earlier at Sonnblick (Kasper and Puxbaum, 1998) and are due to meteorological conditions. They lead to rather clean conditions in winter and an enhanced influence of boundary layer air in summer, due to vertical mixing. Applying this concept to the results of plastics analyses, the smaller influence of boundary layer air during the colder season leads to lower plastics concentrations, as well as a higher contribution of nanoplastics.

3.2. Source region analysis

Airborne long-range transport of microplastics has already been described as an important transport pathway (Evangeliou et al., 2020; González-Pleiter et al., 2021). To assess whether the episodic occurrence of PE and PP/PPC can be linked with certain source areas, we evaluated source-receptor relationships obtained from FLEXPART modelling. Most of the samples with a contribution of PE and PP/PPC showed source regions above the Atlantic and northern or eastern Europe, some even an influence of North America. Source regions above the Atlantic might point to sea spray as a source of airborne microplastics (Allen et al., 2020). Still, we want to highlight that this feature is not characteristic, as

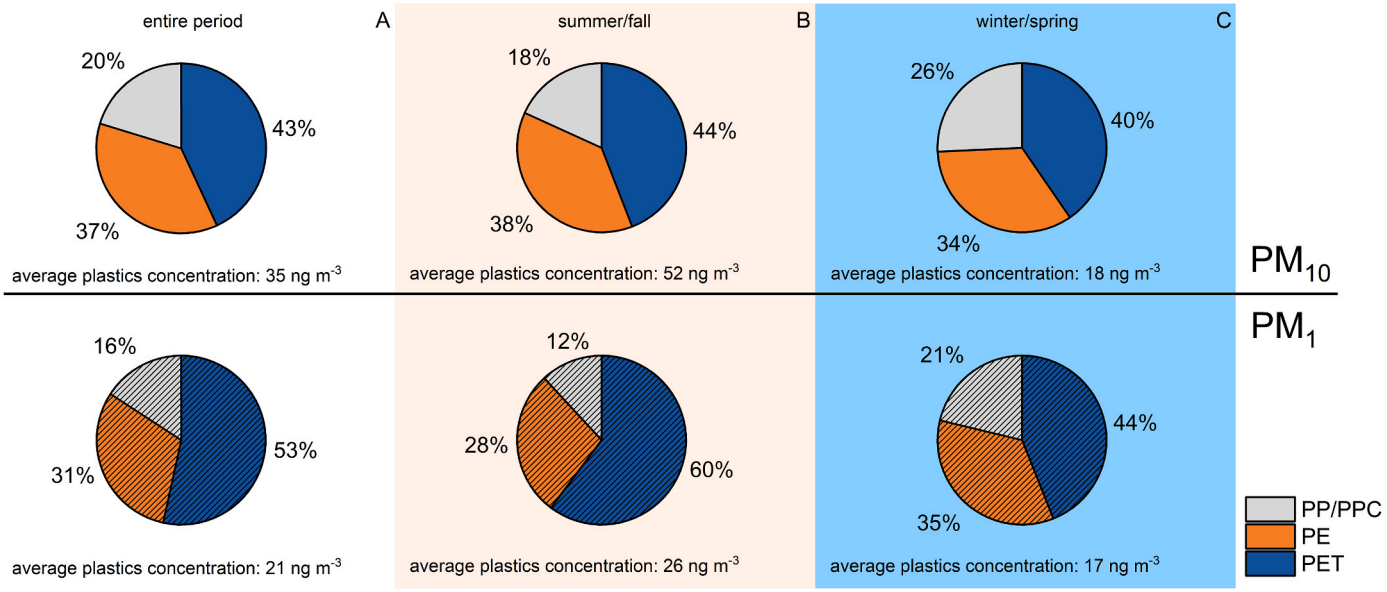

Fig. 2. Average percentage of each plastic type in overall plastics mass (considering PET, PE and PP/PPC) for PM_{10} and PM_1. A: all analysed samples considered; B: summer/fall period; C: winter/spring period.

a number of samples containing only PET show similar source-receptor fields as well. Example SRS maps are given in the Supplement. Overall, an unambiguous assignment of source regions was not possible. This is easily explainable by the rather long sampling intervals, masking more detailed evaluations.

A much more conclusive picture is obtained when the source-receptor relationships are used to interpret the changes in TSP concentrations. Elevated concentrations are always driven by the influence of air masses originating over the Sahara, indicating a long-range transport of mineral dust. Air masses reaching Sonnblick Observatory regularly carry mineral dust (Greilinger et al., 2018). For the observed period, 10 out of the 23 samples could be classified as influenced by mineral dust, based on the FLEXPART calculation, which was in good agreement with a visual inspection of the filters. For high mineral dust loadings, a characteristic reddish colouring is visible on the filter, due to their iron oxide content (Fig. S1 in the Supplement). The 10 filters with influence of mineral dust are distributed rather equally between the summer/fall and winter/spring periods (summer/fall: 6; winter/spring: 4). Within the summer/fall period, filters with and without mineral dust alternate more frequently due to many smaller mineral dust events, while in the winter/spring period, mineral dust events appear mainly near the end of the period. In March 2022, an intense long-range transport event of mineral dust to Europe occurred (Gomes et al., 2022; Qor-el-aine et al., 2022).

The data shown in Fig. 1 suggests that filters influenced by mineral dust (classification based on TSP concentration, weaker events (up to 10 μg m^{-3}) indicated with *, strong events (above 30 μg m^{-3}) indicated with **) do not show elevated plastics concentrations compared to the weekly filters before and after. In the summer/fall period, the highest plastics concentrations occur in two consecutive weeks, while only in the second week a mineral dust event occurred at Sonnblick Observatory, suggesting that mineral dust does not influence the plastics concentration within our observation period. This is also true for the winter/spring period. This contrasts with a recent publication mentioning dust storms as a potential means of transport for microplastics in the atmosphere (Abbasi et al., 2022). However, the experimental set-up described by Abbasi et al. (2022) refers to much shorter distances of transport. Overall, mineral dust does not act as a noticeable transport vehicle for plastics at our site.

The sample collected between 24.03.22 and 31.03.22 is special. Being classified as influenced by mineral dust, it shows very high concentrations of PET, PE and PP/PPC for this period. Additionally, this filter showed elevated concentrations of levoglucosan and EC. It was collected at the end of March 2022, a period with a high number of wildfires in Austria and surrounding countries (European Commission, 2023), which also becomes visible via both elevated mixing ratios of carbon monoxide and a marked correlation of carbon monoxide and TSP concentrations (Schauer et al., 2016; Wigder et al., 2013) at Sonnblick Observatory. Hale et al. (2020) mention that wildfires have been inadequately evaluated as a source of microplastics and additives. Here we find high plastics concentrations in combination with smoke from wildfires. Still, no causality can be derived from the present analysis. Other filters showing elevated plastics concentrations (e.g., in July 2021) could not be linked to a concurrent influence of fires.

3.3. Spearman rank correlation

Spearman rank correlation was used to identify possible relationships of different aerosol constituents and overall aerosol mass, expressed by TSP. Due to the low number of filters containing PE or PP/PPC, only PET was considered as plastics representative, furthermore the aerosol constituents levoglucosan, arabitol, EC, OM, SO_4^{2-}, NH_4^+, NO_3^-, Ca^{2+} and Fe were evaluated. TSP showed significant correlation coefficients (level of significance = 0.05) with all parameters except levoglucosan. This remains valid for both, the PM_{10} and the PM_1 fraction. Three filters were affected by pronounced loadings of mineral dust (marked with ** in Fig. 1, classification: section 3.2.). Consequently, elevated concentrations of TSP as well as Ca^{2+} and Fe dominate several of the correlations. Hence, we used the standardized data set for further evaluation. Furthermore, the filter sampled during a period with a high number of wildfires was excluded for further evaluations, as elevated concentrations of levoglucosan and NH_4^+ would lead to a bias. For clarity the data point is included in the scatter plots (highlighted in black) but excluded from correlation analysis. Correlations are shown in Fig. 3 and Table 1, whereas only correlations of PET with other constituents are discussed in more detail below.

For the standardized data set of PM_{10}, significant correlations (level of significance = 0.05) were obtained for PET and the carbonaceous fractions (EC and OM), arabitol as well as the inorganic ions SO_4^{2-}, NO_3^- and NH_4^+. EC, SO_4^{2-}, NO_3^- and NH_4^+ represent anthropogenic tracers, making a correlation with anthropogenic microplastics quite comprehensible. Correlations were most pronounced for EC and OM. As mentioned earlier, plastics represent a minor constituent of OM, with an average share of 2%. Furthermore, a significant correlation between PET and arabitol was found. Arabitol is used as a tracer for bioaerosols like fungal spores (Bauer et al., 2008). As vegetation is negligible in the direct vicinity of the sampling site, elevated contribution of arabitol is caused by boundary layer air that reaches crest height loaded with anthropogenic pollutants. No significant correlation was found for PET and Ca^{2+} or Fe, affirming the assumption that the occurrence of mineral dust does not influence ambient plastics concentrations at least for PET at our site. Furthermore, no significant correlation was found for PET and levoglucosan. Levoglucosan is used as a tracer for wood combustion, e.g., its use for energy generation and heating (Schmidl et al., 2008). The scatter plot (Fig. 3) indicates two groups of data points which reflect the winter/spring and summer/fall periods. Evaluating these seasons separately, the correlation between levoglucosan and PET becomes significant. The concentrations of levoglucosan in boundary air layer build up in the cold season (Caseiro et al., 2009) and can then be regarded as an anthropogenic marker, just as the microplastics. In the warm season, ground level concentrations of levoglucosan are much lower, leading to a different pattern. Besides levoglucosan, a separation of data points according to season is also visible for arabitol. Arabitol concentrations are very low during wintertime, leading to negligible concentrations during the cold season.

4. Conclusion

We report a first data set for ambient concentrations of fine micro- and nanoplastics in air for the Global Atmosphere Watch station Sonnblick Observatory. While PET was found to be ubiquitous, PE and PP/PPC occurred more episodically and with higher uncertainties. PS, PVC and tire wear particles were rarely determined and if so with quite low concentrations. Considering the three main plastic types, average plastics concentrations of weekly sampling were 35 and 21 ng m^{-3} with maximum concentrations of 165 and 113 ng m^{-3} for PM_{10} and PM_1, respectively. While the concentrations at the background site were lower than in an urban environment, the average contribution of the analysed polymers to organic matter at both sites was comparable.

A comparison of plastics concentrations in the summer/fall and winter/spring period showed higher average concentrations and an increased presence of fine microplastics (average concentration of plastics in PM_{10} higher by a factor of 2 compared to PM_1) in the warmer period. In the colder period, average plastics concentrations and contribution of different plastic types of both size fractions were comparable, suggesting that plastic particles were mainly present as nanoplastics.

The use of a source-receptor model and TSP mass allowed to classify samples influenced by mineral dust. No statistically significant correlation between plastics concentrations and mineral dust tracers was found, indicating that mineral dust does not function as a transport vehicle for fine micro- and nanoplastics at the site. Significant correlations between

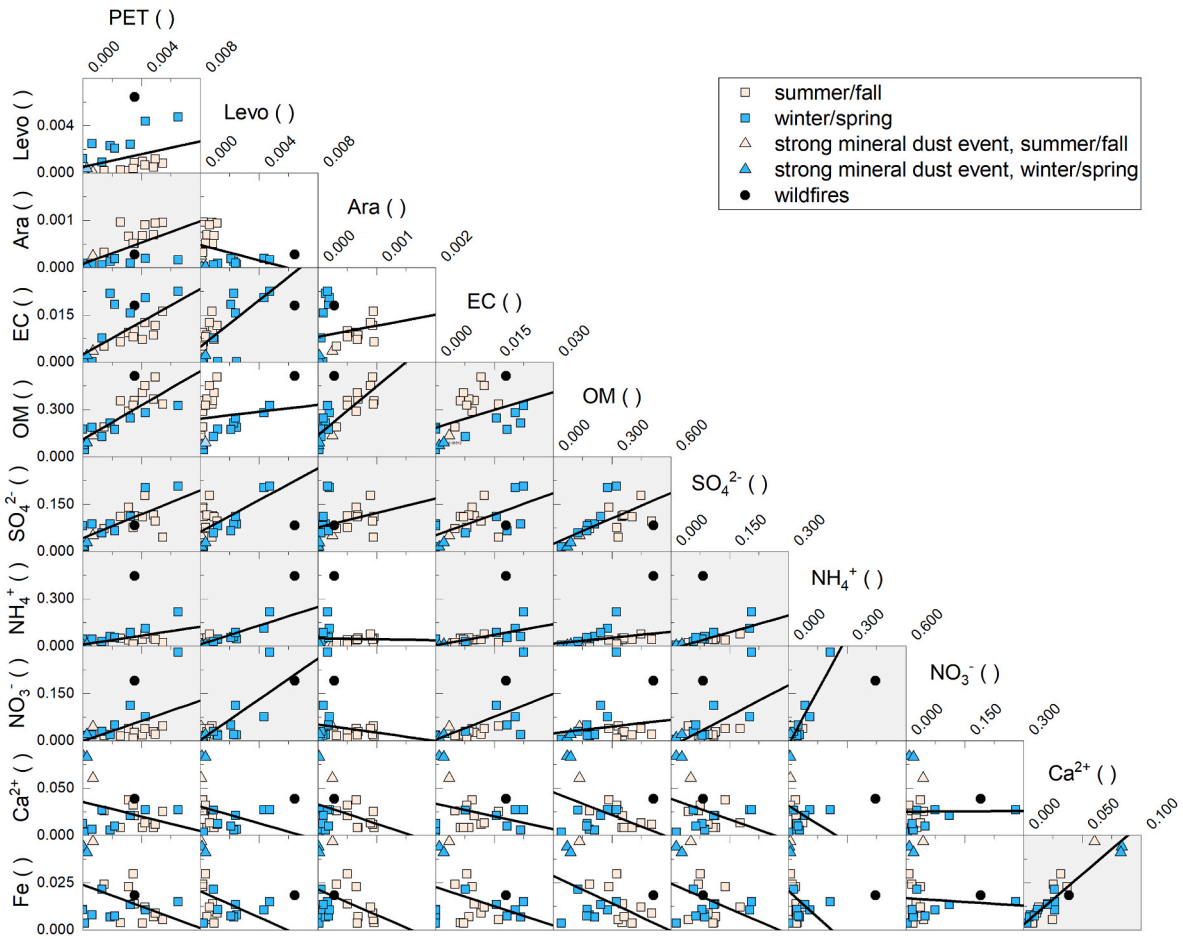

Fig. 3. Scatter plots of various PM_{10} constituents after standardization with TSP mass concentration. Pink: summer/fall period; blue: winter/spring period; triangles: filters of three strongest mineral dust events; circle: filter with influence of wildfires (excluded from statistical evaluation); grey filling: significant correlation (level of significance = 0.05); Levo: levoglucosan; Ara: arabitol. (For interpretation of the references to colour in this figure legend, the reader is referred to the Web version of this article.)

Table 1
Spearman rank correlation coefficients for various PM_{10} constituents after standardization with TSP mass concentration.

	PET	Levo[a]	Ara[b]	EC	OM	SO_4^{2-}	NH_4^+	NO_3^-	Ca^{2+}	Fe
PET	1.00									
Levo[a]	0.359	1.00								
Ara[b]	**0.719**[c]	−0.107	1.00							
EC	**0.762**[c]	**0.552**[c]	0.374	1.00						
OM	**0.836**[c]	0.208	**0.870**[c]	**0.484**[c]	1.00					
SO_4^{2-}	**0.652**[c]	**0.455**[c]	**0.482**[c]	**0.539**[c]	**0.700**[c]	1.00				
NH_4^+	**0.511**[c]	**0.781**[c]	0.222	**0.674**[c]	**0.448**[c]	**0.781**[c]	1.00			
NO_3^-	**0.543**[c]	**0.451**[c]	0.163	**0.724**[c]	0.190	**0.430**[c]	**0.546**[c]	1.00		
Ca^{2+}	−0.048	−0.348	−0.177	0.009	−0.249	−0.143	−0.357	0.251	1.00	
Fe	−0.254	−0.361	−0.320	−0.150	−0.325	−0.161	−0.376	0.091	**0.872**[c]	1.00

[a] Levo: levoglucosan.
[b] Ara: arabitol.
[c] For significant correlations (level of significance = 0.05), coefficients are written in bold.

the PET concentration and the anthropogenic tracers EC, NO_3^-, NH_4^+ and SO_4^{2-} as well as OC and arabitol were found.

CRediT authorship contribution statement

Daniela Kau: Conceptualization, Formal analysis, Investigation, Methodology, Visualization, Writing – original draft, Writing – review & editing. **Dušan Materić:** Data curation, Methodology, Software, Validation, Writing – review & editing. **Rupert Holzinger:** Resources, Software, Writing – review & editing. **Kathrin Baumann-Stanzer:** Formal analysis, Writing – review & editing. **Gerhard Schauer:** Formal analysis, Writing – review & editing. **Anne Kasper-Giebl:** Conceptualization, Resources, Supervision, Writing – original draft, Writing – review & editing.

Declaration of competing interest

The authors declare that they have no known competing financial interests or personal relationships that could have appeared to influence the work reported in this paper.

Data availability

Data used for the evaluation of ambient microplastics concentrations was uploaded to TU Wien Data Repository (https://doi.org/10.48436/qfpa8-ga860).

Acknowledgements/Financial Support

The research stay of Daniela Kau at Utrecht University was financed by the Christiana Hörbiger Award 2021. ICP-OES analyses were conducted within the research group Inorganic Trace Analysis (TU Wien) and MAPAG Materialprüfungs GmbH. Special thanks go to Thomas Riedelberger, Andjela Vukićević, Michaela Zuckerhut and Karoline Rieger for their contribution in sample preparation and chemical analyses and to the technicians at Sonnblick Observatory for sample collection. The authors acknowledge TU Wien Bibliothek for financial support through its Open Access Funding Programme.

Appendix A. Supplementary data

Supplementary data to this article can be found online at https://doi.org/10.1016/j.chemosphere.2024.141410.

References

Abbasi, S., Turner, A., 2021. Dry and wet deposition of microplastics in a semi-arid region (Shiraz, Iran). Sci. Total Environ. 786, 147358.
Abbasi, S., Rezaei, M., Ahmadi, F., Turner, A., 2022. Atmospheric transport of microplastics during a dust storm. Chemosphere 292, 133456.
Akhbarizadeh, R., Dobaradaran, S., Torkmahalleh, M.A., Saeedi, R., Aibaghi, R., Ghasemi, F.F., 2021. Suspended fine particulate matter (PM2. 5), microplastics (MPs), and polycyclic aromatic hydrocarbons (PAHs) in air: their possible relationships and health implications. Environ. Res. 192, 110339.
Allen, S., Allen, D., Moss, K., Le Roux, G., Phoenix, V.R., Sonke, J.E., 2020. Examination of the ocean as a source for atmospheric microplastics. PLoS One 15, e0232746.
Allen, S., Materić, D., Allen, D., Macdonald, A., Holzinger, R., Le Roux, G., Phoenix, V.R., 2022. An early comparison of nano to microplastic mass in a remote catchment's atmospheric deposition. J. Hazard. Mat. Adv. 7, 100104.
Andrady, A.L., 2015. Persistence of plastic litter in the oceans. Marine anthropogenic litter 57–72.
Araujo, C.F., Nolasco, M.M., Ribeiro, A.M., Ribeiro-Claro, P.J., 2018. Identification of microplastics using Raman spectroscopy: Latest developments and future prospects. Water Res. 142, 426–440.
Bauer, H., Claeys, M., Vermeylen, R., Schueller, E., Weinke, G., Berger, A., Puxbaum, H., 2008. Arabitol and mannitol as tracers for the quantification of airborne fungal spores. Atmos. Environ. 42, 588–593.
Baumann-Stanzer, K., Greilinger, M., Kasper-Giebl, A., Flandorfer, C., Hieden, A., Lotteraner, C., Ortner, M., Vergeiner, J., Schauer, G., Piringer, M., 2019. Evaluation of WRF-chem model forecasts of a prolonged saharan dust episode over the eastern alps. Aerosol Air Qual. Res. 19, 1226–1240.
Bergmann, M., Mützel, S., Primpke, S., Tekman, M.B., Trachsel, J., Gerdts, G., 2019. White and wonderful? Microplastics prevail in snow from the Alps to the Arctic. Sci. Adv. 5, eaax1157.
Biber, N.F., Foggo, A., Thompson, R.C., 2019. Characterising the deterioration of different plastics in air and seawater. Mar. Pollut. Bull. 141, 595–602.
Brahney, J., Hallerud, M., Heim, E., Hahnenberger, M., Sukumaran, S., 2020. Plastic rain in protected areas of the United States. Science 368, 1257–1260.
Cabrera, M., Valencia, B.G., Lucas-Solis, O., Calero, J.L., Maisincho, L., Conicelli, B., Moulatlet, G.M., Capparelli, M.V., 2020. A new method for microplastic sampling and isolation in mountain glaciers: a case study of one antisana glacier, Ecuadorian Andes. Case Stud. Chem. Environ. Eng. 2, 100051.
Cai, L., Wang, J., Peng, J., Wu, Z., Tan, X., 2018. Observation of the degradation of three types of plastic pellets exposed to UV irradiation in three different environments. Sci. Total Environ. 628, 740–747.
Caseiro, A., Bauer, H., Schmidl, C., Pio, C.A., Puxbaum, H., 2009. Wood burning impact on PM10 in three Austrian regions. Atmos. Environ. 43, 2186–2195.
Cavalli, F., Viana, M., Yttri, K.E., Genberg, J., Putaud, J.P., 2010. Toward a standardised thermal-optical protocol for measuring atmospheric organic and elemental carbon: the EUSAAR protocol. Atmos. Meas. Tech. 3, 79–89.
Chen, G., Feng, Q., Wang, J., 2020. Mini-review of microplastics in the atmosphere and their risks to humans. Sci. Total Environ. 703, 135504.
Chen, Y., Wen, D., Pei, J., Fei, Y., Ouyang, D., Zhang, H., Luo, Y., 2020. Identification and quantification of microplastics using Fourier-transform infrared spectroscopy: current status and future prospects. Curr. Opin. Environ. Sci. Health 18, 14–19.
Chinaglia, S., Tosin, M., Degli-Innocenti, F., 2018. Biodegradation rate of biodegradable plastics at molecular level. Polym. Degrad. Stabil. 147, 237–244.
Cox, K.D., Covernton, G.A., Davies, H.L., Dower, J.F., Juanes, F., Dudas, S.E., 2019. Human consumption of microplastics. Envir. sci. technol. 53, 7068–7074.
DIN e.V.: DIN CEN ISO/TR 21960, 2021. Kunststoffe in der Umwelt - Aktueller Wissensstand und Methodik (ISO/TR 21960:2020); Englische Fassung CEN ISO/TR 21960:2020. Beuth Verlag GmbH, Berlin.
European Commission, Joint Research Centre, San-Miguel-Ayanz, J., Durrant, T., Boca, R., et al., 2023. Advance Report on Forest Fires in Europe, Middle East and North Africa 2022. Publications Office of the European Union. https://data.europa.eu/doi/10.2760/091540.
Evangeliou, N., Grythe, H., Klimont, Z., Heyes, C., Eckhardt, S., Lopez-Aparicio, S., Stohl, A., 2020. Atmospheric transport is a major pathway of microplastics to remote regions. Nat. comm. 11, 3381.
Gomes, J., Esteves, H., Rente, L., 2022. Influence of an extreme saharan dust event on the air quality of the west region of Portugal. Gas 2, 74–84.
González-Pleiter, M., Edo, C., Aguilera, Á., Viúdez-Moreiras, D., Pulido-Reyes, G., González-Toril, E., Osuna, S., de Diego-Castilla, G., Leganés, F., Fernández-Piñas, F., Rosal, R., 2021. Occurrence and transport of microplastics sampled within and above the planetary boundary layer. Sci. Total Environ. 761, 143213.
Greilinger, M., Schauer, G., Baumann-Stanzer, K., Skomorowski, P., Schöner, W., Kasper-Giebl, A., 2018. Contribution of Saharan dust to ion deposition loads of high alpine snow packs in Austria (1987–2017). Front. Earth Sci. 6, 126.
Hale, R.C., Seeley, M.E., La Guardia, M.J., Mai, L., Zeng, E.Y., 2020. A global perspective on microplastics. J. Geophys. Res-Oceans 125, e2018JC014719.
Holzinger, R., 2015. PTRwid: a new widget tool for processing PTR-TOF-MS data. Atmos. Meas. Tech. 8, 3903–3922.
Holzinger, R., Acton, W.J.F., Bloss, W.J., Breitenlechner, M., Crilley, L.R., Dusanter, S., Gonin, M., Gros, V., Keutsch, F.N., Kiendler-Scharr, A., Kramer, L.J., Krechmer, J.E., Languille, B., Locoge, N., Lopez-Hilfiker, F., Materić, D., Moreno, S., Nemitz, E., Quéléver, L.L.J., Sarda Esteve, R., Sauvage, S., Schallhart, S., Sommariva, R., Tillmann, R., Wedel, S., Worton, D.R., Xu, K., Zaytsev, A., 2019. Validity and limitations of simple reaction kinetics to calculate concentrations of organic compounds from ion counts in PTR-MS. Atmos. Meas. Tech. 12, 6193–6208.
Ivleva, N.P., 2021. Chemical analysis of microplastics and nanoplastics: challenges, advanced methods, and perspectives. Chem. Rev. 121, 11886–11936.
Jiang, J., Ren, H., Wang, X., Liu, B., 2024. Pollution characteristics and potential health effects of airborne microplastics and culturable microorganisms during urban haze in Harbin, China. Bioresour. Technol. 393, 130132.
Kacprzak, S., Tijing, L.D., 2022. Microplastics in indoor environment: sources, mitigation and fate. J. Environ. Chem. Eng. 10, 107359.
Kanhai, L.D.K., Gardfeldt, K., Krumpen, T., Thompson, R.C., O'Connor, I., 2020. Microplastics in sea ice and seawater beneath ice floes from the Arctic Ocean. Sci. rep.-UK 10, 5004.
Kasper, A., Puxbaum, H., 1998. Seasonal variation of SO2, HNO3, NH3 and selected aerosol components at Sonnblick (3106 m asl). Atmos. Environ. 32, 3925–3939.
Kirchsteiger, B., Materić, D., Happenhofer, F., Holzinger, R., Kasper-Giebl, A., 2023. Fine micro-and nanoplastics particles (PM2. 5) in urban air and their relation to polycyclic aromatic hydrocarbons. Atmos. Environ. 301, 119670.
Kumar, M., Xiong, X., He, M., Tsang, D.C., Gupta, J., Khan, E., Harrad, S., Hou, D., Ok, Y. S., Bolan, N.S., 2020. Microplastics as pollutants in agricultural soils. Environ. Pollut. 265, 114980.
Lebreton, L., Andrady, A., 2019. Future scenarios of global plastic waste generation and disposal. Palgrave Commun 5, 1–11.
Materić, D., Peacock, M., Kent, M., Cook, S., Gauci, V., Röckmann, T., Holzinger, R., 2017. Characterisation of the semi-volatile component of dissolved organic matter by thermal desorption–proton transfer reaction–mass spectrometry. Sci. rep.-UK 7, 15936.
Materić, D., Ludewig, E., Xu, K., Röckmann, T., Holzinger, R., 2019. Brief communication: analysis of organic matter in surface snow by PTR-MS–implications for dry deposition dynamics in the Alps. Cryosphere 13, 297–307.
Materić, D., Kasper-Giebl, A., Kau, D., Anten, M., Greilinger, M., Ludewig, E., van Sebille, E., Röckmann, T., Holzinger, R., 2020. Micro-and nanoplastics in alpine snow: a new method for chemical identification and (semi) quantification in the nanogram range. Environ. Sci. Technol. 54, 2353–2359.
Materić, D., Ludewig, E., Brunner, D., Röckmann, T., Holzinger, R., 2021. Nanoplastics transport to the remote, high-altitude Alps. Environ. Pollut. 288, 117697.
Materić, D., Kjær, H.A., Vallelonga, P., Tison, J.L., Röckmann, T., Holzinger, R., 2022. Nanoplastics measurements in Northern and Southern polar ice. Environ. Res. 208, 112741.
Napper, I.E., Thompson, R.C., 2019. Environmental deterioration of biodegradable, oxo-biodegradable, compostable, and conventional plastic carrier bags in the sea, soil, and open-air over a 3-year period. Environ. Sci. Technol. 53, 4775–4783.
OECD, 2022. Global Plastics Outlook: Economic Drivers, Environmental Impacts and Policy Options. OECD Publishing, Paris. https://doi.org/10.1787/de747aef-en.
Padha, S., Kumar, R., Dhar, A., Sharma, P., 2022. Microplastic pollution in mountain terrains and foothills: a review on source, extraction, and distribution of microplastics in remote areas. Environ. Res. 207, 112232.
Pastorino, P., Pizzul, E., Bertoli, M., Anselmi, S., Kuśće, M., Menconi, V., Prearo, M., Renzi, M., 2021. First insights into plastic and microplastic occurrence in biotic and abiotic compartments, and snow from a high-mountain lake (Carnic Alps). Chemosphere 265, 129121.
PlasticsEurope, 2012. Plastics - the Facts 2012, Plastics Europe. Belgium.
PlasticsEurope, 2022. Plastics - the Facts 2022, Plastics Europe AISBL. Belgium.
Prata, J.C., 2018. Airborne microplastics: consequences to human health? Environ. Pollut. 234, 115–126.
Puxbaum, H., Caseiro, A., Sánchez-Ochoa, A., Kasper-Giebl, A., Claeys, M., Gelencsér, A., Legrand, M., Preunkert, S., Pio, C., 2007. Levoglucosan levels at background sites in Europe for assessing the impact of biomass combustion on the European aerosol background. J. Geophys. Res. Atmos. 112.

Qor-El-Aine, A., Béres, A., Géczi, G., 2022. Case study of the saharan dust effects on PM10 and PM2. 5 concentrations in Budapest in March 2022. Journal of Central European Green Innovation 10, 67–78.
Rodrigues, M.O., Abrantes, N., Gonçalves, F.J.M., Nogueira, H., Marques, J.C., Gonçalves, A.M.M., 2018. Spatial and temporal distribution of microplastics in water and sediments of a freshwater system (Antuã River, Portugal). Sci. Total Environ. 633, 1549–1559.
Schauer, G., Kasper-Giebl, A., Močnik, G., 2016. Increased PM concentrations during a combined wildfire and Saharan dust event observed at high-altitude Sonnblick Observatory, Austria. Aerosol Air Qual. Res. 16, 542–554.
Schmidl, C., Marr, I.L., Caseiro, A., Kotianová, P., Berner, A., Bauer, H., Kasper-Giebl, A., Puxbaum, H., 2008. Chemical characterisation of fine particle emissions from wood stove combustion of common woods growing in mid-European Alpine regions. Atmos. Environ. 42, 126–141.
Stohl, A., Eckhardt, S., Forster, C., James, P., Spichtinger, N., Seibert, P., 2002. A replacement for simple back trajectory calculations in the interpretation of atmospheric trace substance measurements. Atmos. Environ. 36, 4635–4648.
Wang, X., Li, C., Liu, K., Zhu, L., Song, Z., Li, D., 2020. Atmospheric microplastic over the South China sea and East Indian ocean: abundance, distribution and source. J. Hazard Mater. 389, 121846.
Wang, X., Wei, N., Liu, K., Zhu, L., Li, C., Zong, C., Li, D., 2022. Exponential decrease of airborne microplastics: from megacity to open ocean. Sci. Total Environ. 849, 157702.
Wigder, N.L., Jaffe, D.A., Saketa, F.A., 2013. Ozone and particulate matter enhancements from regional wildfires observed at Mount Bachelor during 2004–2011. Atmos. Environ. 75, 24–31.
Wright, S.L., Levermore, J.M., Kelly, F.J., 2019. Raman spectral imaging for the detection of inhalable microplastics in ambient particulate matter samples. Environ. Sci. Technol. 53, 8947–8956.